Polyhedron 158 (2019) 1–7

Contents lists available at ScienceDirect

Polyhedron

journal homepage: www.elsevier.com/locate/poly

Preparation of U(IV) κ^1-amidinate complexes by nitrile metathesis

Caleb J. Tatebe, Tyler S. Collins, Grant Reed Barnett, Matthias Zeller, Suzanne C. Bart *

H.C. Brown Laboratory, Department of Chemistry, Purdue University, West Lafayette, IN 47907, United States

ARTICLE INFO

Article history:
Received 30 August 2018
Accepted 16 October 2018
Available online 28 October 2018

This article is dedicated to Professor William D. Jones on the occasion of his 65th birthday.

Keywords:
Uranium
Cycloaddition
Scorpionate ligands
Actinide chemistry

ABSTRACT

Treating U(IV) imido compounds, Tp^*_2U(N-*p*-methoxyphenyl) (**2-OMe**) and Tp^*_2U(N-*p*Tol) (**2-*p*Tol**), with benzonitrile or 4-cyanopyridine results in unusual products of multiple bond metathesis ([2π + 2π]-cycloaddition and [2π + 2π]-cycloreversion). ^{1}H and ^{11}B NMR, infrared, and electronic absorption spectroscopic analyses provides evidence of tetravalent uranium compounds, while X-ray crystallography confirmed molecular structures to be Tp^*_2U[=N—C(=N-*p*OMePh)pyr] (**3-py**), Tp^*_2U[=N—C(=N-*p*OMePh)Ph] (**3-Ph**), Tp^*_2U[=N—C(=N-*p*Tol)pyr] (**4-py**), Tp^*_2U[=N—C(=N-*p*Tol)Ph] (**4-Ph**), Tp^*_2U[=N—C(=N-*p*OMePh)*p*-CNPh] (**5-OMe**), and Tp^*_2U[=N—C(=N-*p*Tol)*p*-CNPh] (**5-Tol**). Previous examples of actinide imidos treated with nitriles resulted in cyclometallated products; thus, the compounds reported represent divergent chemistry in that an κ^1-amidinate ligand is formed through [2π + 2π]-cycloaddition and [2π + 2π]-cycloreversion.

1. Introduction

Small molecule activation has been extensively studied within the actinide community due to the highly reducing nature of these elements [1–3]. Making use of actinide-element multiple bonds is a strategy with diverse reaction pathways dictated by the steric environment [4,5]. Like early transition metal counterparts, actinide-element multiple bonds can undergo [2π + 2π]-cycloaddition and [2π + 2π]-cycloreversion, facilitating a direct comparison of d- versus f-block reactivity.

Such reactivity has been studied for the early actinides – an important example of actinide (uranium, thorium) cycloaddition was reported by Eisen and co-workers [6,7], who proposed this as an intermediate step during catalytic alkyne hydroamination. The κ^2-enamine ligands were later isolated by Andersen (U) [8] and Zi et al. (Th) [9,10], as the product of alkyne addition to An (IV) imido compounds, respectively. Boncella [11] and Meyer [12] have shown [2π + 2π]-cycloaddition of uranium imidos with aryl isocyanates results in κ^2-ureato ligands for both U(IV) and U (V) compounds. Similar examples of κ^2-bound ligands have been isolated for Th imidos when treated with azides [13], carbodiimides [14], and nitriles [15].

Boncella and co-workers have demonstrated that U(VI) bis (imido) compounds can sequentially exchange imido groups when treated with an aryl isocyanate via [2π + 2π]-cycloaddition and concomitant [2π + 2π]-cycloreversion [16]. This is surprising given the high oxophilicity of uranium [17]. More expected are reactions that proceed through multiple bond metathesis pathways to form Th [9] and U [18] oxo compounds.

Multiple bond metathesis, the combination of [2π + 2π]-cycloaddition and [2π + 2π]-cycloreversion, of uranium imido compounds has been a subject of recent interest in our laboratory as well. Using tetravalent Tp^*_2U(N-R) (Tp^* = hydrotris(3,5-dimethylpyrazolyl) borate; R = Ph, Mes, Ad), the corresponding U(IV) oxo, Tp^*_2UO, can be prepared via treatment with *p*-tolualdehyde with simultaneous release of the substituted imine [19]. The analogous [2π + 2π] cycloaddition chemistry occurs with alkynes and diazoalkanes, where both small molecules yield metallacyclic uranium derivatives [20]. More recently, we have reported [2π + 2π] cycloaddition products of reactions with a series of isocyanates, PhNCE (E = O, S, Se), where different κ^2-chalcogen-ureato derivatives are isolated [21]. Here, we report the reactivity of uranium imidos with nitriles that is divergent from previously reported studies. These resulting products are a new class of sterically-hindered κ^1-amidinate compounds that have undergone full spectroscopic and structural characterization to confirm this unique reactivity.

2. Material and methods

2.1. General considerations

All air- and moisture-sensitive manipulations were performed using standard Schlenk techniques or in an MBraun inert

* Corresponding author.
E-mail address: sbart@purdue.edu (S.C. Bart).

https://doi.org/10.1016/j.poly.2018.10.042
0277-5387/

atmosphere drybox with an atmosphere of purified nitrogen. The MBraun drybox was equipped with a cold well designed for freezing samples in liquid nitrogen as well as two −35 °C freezers for cooling samples and crystallizations. Solvents for sensitive manipulations were dried and deoxygenated based on literature procedures using a Seca solvent purification system [22]. Benzene-d_6 was purchased from Cambridge Isotope Laboratories, dried with molecular sieves and sodium, and degassed by three freeze–pump–thaw cycles. 4-cyanopyridine and terephthalonitrile were purchased from Acros Organics and used as received. Benzonitrile was purchased from Sigma-Aldrich and degassed by three freeze–pumpthaw cycles before use. Potassium graphite [23], Tp^*_2UI (**1-I**) [24], $Tp^*_2UCH_2Ph$ (**1-Bn**) [25], and Tp^*_2U(N-*p*Tol) (**2-*p*Tol**) [21], were prepared per literature procedures. An adapted method was used for the synthesis of *p*-methoxyphenyl azide [26].

^{1}H NMR spectra were recorded on a Varian Inova 300 spectrometer operating at 299.992 MHz. ^{11}B NMR spectra were recorded on a Varian Inova 300 spectrometer operating at a frequency of 96.24 MHz. All chemical shifts are reported relative to the peak for $SiMe_4$, using ^{1}H (residual) chemical shifts of the solvent (C_6D_6: 7.16 ppm) as a secondary standard. ^{11}B chemical shifts are reported relative to the peak for $BF_3{\cdot}Et_2O$ (0.0 ppm). The spectra for paramagnetic molecules were obtained by using an acquisition time of 0.5 s, thus the peak widths reported have an error of ±2 Hz. For paramagnetic molecules, the ^{1}H NMR data are reported with the chemical shift, followed by the peak width at half height in Hertz, the integration value, and, where possible, the peak assignment. Elemental analyses were performed by Midwest Microlab, LLC (Indianapolis, Indiana). Solid state infrared spectra were recorded using a Thermo Nicolet 6700 spectrophotometer; samples were made by crushing the solids, mixing with dry KBr, and pressing into a pellet. Electronic absorption spectroscopic measurements were recorded at ambient temperature in sealed 1 cm quartz cuvettes with a Cary 6000i UV–Vis-NIR spectrophotometer.

Single crystals of **3-Ph**, **3-py**, **4-py**, **5-OMe** and **5-Tol** suitable for X-ray diffraction, were coated with poly(isobutylene) oil in a drybox and quickly transferred to the goniometer head of a Bruker AXS D8 Quest diffractometer with a fixed chi angle, a sealed tube fine focus X-ray tube, single crystal curved graphite incident beam monochromator and a Photon100 CMOS area detector. Examination and data collection were performed with Mo Kα radiation (λ = 0.71073 Å) (**3-Ph**, **3-py**, **4-py**, **5-Tol**) or Cu Kα radiation (λ = 1.5406 Å) (**5-OMe**). Data were collected, reflections were indexed and processed, and the files scaled and corrected for absorption using APEX3 [27]. Additional details for each compound are given in the SI.

*2.1.1. Synthesis of $Tp^*_2U(=N\text{-}pOMeC_6H_4)$ (**2-OMe**).*

To a 20 mL scintillation vial, **1-Bn** (0.750 g, 0.812 mmol) was dissolved in 15 mL THF. To this green solution, *p*-methoxyphenyl azide (0.121 g, 0.812 mmol) was injected, which immediately produced effervescence and color change to deep red. After 5 minutes, volatiles were removed *in vacuo*, affording a red-violet powder. To remove any resulting bibenzyl, this powder was washed with *n*-pentane (3 × 10 mL) and dried again, affording a red-violet powder which is assigned as Tp^*_2U(N-*p*OMeC$_6$H$_4$) (**2-OMe**) (0.726 g, 0.764 mmol, 94% yield).

Elemental analysis of $C_{37}H_{51}B_2N_{13}OU$: Calculated: C, 46.61; H, 5.39; N, 19.10. Experimental: C, 46.00; H, 5.42; N, 17.88. ^{1}H NMR (benzene-d_6, ambient temperature): δ = −20.98 (3, 2H, Tp* B-*H*), −6.80 (4, 18H, Tp*-C*H*$_3$), 2.85 (30, 18H, Tp*-C*H*$_3$), 5.48 (8, 6H, Tp*-C*H*), 21.18 (2, 3H, -OC*H*$_3$), 52.80 (21, 2H, Ar-*H*), 77.82 (21, 2H, Ar-*H*). ^{11}B NMR (benzene-d_6, ambient temperature): δ = −66. IR (KBr pellet): $\nu_{B\text{-}H}$ = 2556, 2525 cm^{-1}.

*2.1.2. Alternate synthesis of **2-OMe***

A 20 mL scintillation vial was charged with **1-I** (1.000 g, 1.042 mmol) in 15 mL THF. *p*-Methoxyphenyl azide (0.155 g, 1.042 mmol) and KC_8 (0.155 g, 1.147 mmol) were added to the dark blue solution, which resulted in effervescence and darkening of the solution. After 1 h, KI and graphite were removed by filtration over Celite. The solution was then concentrated under reduced pressure, affording a red-violet powder. This solid was washed with *n*-pentane (3 × 15 mL) and dried, resulting in the isolation of **2-OMe** (0.825 g, 0.865 mmol, 83% yield).

2.1.3. Synthesis of $Tp^*_2U[=N\text{—}C(=N(p\text{-}RPh)(Ar)]$.

In a 20 mL scintillation vial, Tp^*_2U(N-*p*-RPh) (R = OMe: 0.120 g, 0.126 mmol; CH_3: 0.120 g, 0.128 mmol) was dissolved in 8 mL THF. To this deep red solution, one equivalent of nitrile (R = OMe: benzonitrile: 13.0 μL; 4-cyanopyridine: 0.013 g, 0.126 mmol; R = CH_3: benzonitrile: 13.2 μL; 4-cyanopyridine: 0.013 g) was added. Within five minutes of stirring, the solutions became a red-orange color, at which point, volatiles were removed *in vacuo*. The resulting orange powders were washed with *n*-pentane (2 × 5 mL) and subsequently dried affording in orange powders assigned as Tp^*_2U[=NC(N-*p*RPh)-Ar] (R = OMe, Ar = Ph (**3-Ph**) 0.105 g, 0.099 mmol, 79% yield; py (**3-py**), 0.111 g, 0.104 mmol, 83% yield; R = CH_3, Ar = Ph (**4-Ph**), 0.100 g, 0.096 mmol, 75% yield; py (**4-py**), 0.104 g, 0.100 mmol, 78% yield). Single crystals were obtained at −35 °C by layering *n*-pentane into a concentrated diethyl ether solution (5:1 ratio) (**3-py**), vapor diffusion of diethyl ether into toluene (**3-Ph**), or concentrated solution of diethyl ether (**4-py**).

2.1.3.1. 3-Ph. Elemental Analysis of $C_{44}H_{56}B_2N_{14}OU$: Calculated: C, 50.01; H, 5.34; N, 18.56. Experimental: C, 49.87; H, 5.77; N, 18.58. ^{1}H NMR (benzene-d_6, ambient temperature): δ = −81.54 (50, 3H, Tp*-C*H*$_3$), −77.93 (15, 3H, Tp*-C*H*$_3$), −28.85 (5, 1H, Tp* B-*H*), −24.96 (3, 1H, Tp* B-*H*), −20.71 (22, 1H, Tp*-C*H*), −19.92 (8, 1H, Tp*-C*H*), −18.81 (7, 3H, Tp*-C*H*$_3$), −18.85 (10, 3H, Tp*-C*H*$_3$), −14.66 (19, 3H, Tp*-C*H*$_3$), -12.43 (9, 3H, Tp*-C*H*$_3$), −6.91 (9, 1H, Tp*-C*H*), −6.83 (4, 1H, Tp*-C*H*), −5.32 (8, 1H, Tp*-C*H*), −3.25 (3, 3H, Tp*-C*H*$_3$), −2.57 (48, 2H, Ar-*H*), 5.36 (9, 3H, *p*OC*H*$_3$), 7.35 (6, 3H, Tp*-C*H*$_3$), 16.82 (25, 2H, Ar-*H*), 18.98 (53, 3H, Tp*-C*H*$_3$), 22.43 (70, 3H, Tp*-C*H*$_3$), 37.70 (23, 2H, Ar-*H*), 41.64 (7, 1H, Tp*-C*H*), 41.75 (7, 1H, Tp*-C*H*), 49.30 (25, 2H, Ar-*H*), 64.95 (75, 3H, Tp*-C*H*$_3$), 73.16 (19, 3H, Tp*-C*H*$_3$). ^{11}B NMR (benzene-d_6, ambient temperature): δ = −86, −76. IR (KBr pellet): $\nu_{B\text{-}H}$ = 2553, 2521 cm^{-1}.

2.1.3.2. 3-py. Elemental Analysis of $C_{43}H_{55}B_2N_{15}OU$: Calculated: C, 48.83; H, 5.24; N, 19.86. Experimental: C, 49.91; H, 5.80; N, 20.18. ^{1}H NMR (benzene-d_6, ambient temperature): δ = −81.41 (17, 3H, Tp*-C*H*$_3$, −77.81 (18, 3H, Tp*-C*H*$_3$), −28.79 (4, 1H, Tp* B-*H*), −24.88 (3, 1H, Tp* B-*H*), −20.70 (12, 1H, Tp*-C*H*), −19.90 (8, 1H, Tp*-C*H*), −18.80 (10, 3H, Tp*-C*H*$_3$), −18.54 (13, 3H, Tp*-C*H*$_3$), −14.66 (13, 3H, Tp*-C*H*$_3$), −12.43 (9, 3H, Tp*-C*H*$_3$), −6.92 (10, 1H, Tp*-C*H*), −5.32 (12, 1H, Tp*-C*H*), −3.25 (6, 3H, Tp*-C*H*$_3$), −2.56 (17, 2H, Ar-C*H*), 5.32 (10, 3H, OC*H*$_3$), 7.31 (11, 3H, Tp*-C*H*$_3$), 16.81 (24, 2H, Ar-C*H*), 18.94 (21, 3H, Tp*-C*H*$_3$), 22.38 (23, 3H, Tp*-C*H*$_3$), 37.65 (29, 2H, Ar-C*H*), 41.54 (13, 1H, Tp*-C*H*), 41.65 (27, 1H, Tp*-C*H*), 49.31 (13, 2H, Ar-C*H*), 64.79 (42, 3H, Tp*-C*H*$_3$), 73.00 (22, 3H, Tp*-C*H*$_3$). ^{11}B NMR (benzene-d_6, ambient temperature): δ = −86, −75. IR (KBr pellet): $\nu_{B\text{-}H}$ = 2551, 2517 cm^{-1}.

2.1.3.3. 4-Ph. Elemental Analysis of $C_{44}H_{56}B_2N_{14}U$: Calculated: C, 50.78; H, 5.42; N, 18.84. Experimental: C, 49.66; H, 5.53; N, 19.34. ^{1}H NMR (benzene-d_6, ambient temperature): δ = −81.31 (15, 3H, Tp*-C*H*$_3$), −77.72 (16, 3H, Tp*-C*H*$_3$), −28.68 (5, 1H, Tp* B-*H*), −24.84 (4, 1H, Tp* B-*H*), −20.67 (12, 1H, Tp*-C*H*), −19.86 (12, 1H, Tp*-C*H*), −18.77 (9, 3H, Tp*-C*H*$_3$), −18.51 (12, 3H, Tp*-C*H*$_3$), −14.64 (11, 3H, Tp*-C*H*$_3$), −12.41 (9, 3H, Tp*-C*H*$_3$), −6.89 (24, 1H,

Tp*-C*H*), −5.29 (11, 1H, Tp*-C*H*), −3.22 (6, 3H, Tp*-CH_3), −2.54 (14, 2H, Ar-C*H*), 5.32 (9, 3H, *para*-CH_3), 7.32 (9, 3H, Tp*-CH_3), 16.81 (22, 3H, Tp*-CH_3), 18.91 (16, 2H, Ari-C*H*), 37.62 (10, 1H, Tp*-C*H*), 41.51 (10, 1H, Tp*-C*H*), 41.63 (9, 1H, Tp*-C*H*), 49.17 (22, 2H, Ar-C*H*), 64.73 (51, 3H, Tp*-CH_3), 72.96 (19, 3H, Tp*-CH_3). ^{11}B NMR (benzene-d_6, ambient temperature): δ = −82, −76. IR (KBr pellet): $\nu_{B\text{-}H}$ = 2550, 2522 cm^{-1}.

2.1.3.4. 4-py. Elemental Analysis of $C_{43}H_{55}B_2N_{15}U$: Calculated: C, 49.58; H, 5.32; N, 20.17. Experimental: C, 49.05; H, 5.52; N, 19.71. ^{1}H NMR (benzene-d_6, ambient temperature): δ = −82.66 (12, 3H, Tp*-CH_3), −77.25 (13, 3H, Tp*-CH_3), −27.82 (2, 1H, Tp* B-*H*), −25.63 (3, 1H, Tp* B-*H*), −20.44 (8, 4H, Tp*-CH_3 + Tp*-C*H*), −18.75 (7, 3H, Tp*-CH_3), −18.61 (37, 3H, Tp*-CH_3), −14.17 (9, 3H, Tp*-CH_3), −12.84 (19, 3H, Tp*-CH_3), −7.08 (73, 1H, Tp*-C*H*), −5.66 (8, 1H, Tp*-C*H*), −3.99 (47, 3H, Tp*-CH_3), −2.50 (89, 2H, Ar-C*H*), 5.89 (7, 3H, *p*Tol-CH_3), 6.36 (3, 1H, Tp*-C*H*), 8.11 (20, 1H, Tp*-C*H*), 17.20 (18, 2H, Ar-C*H*), 20.01 (98, 3H, Tp*-CH_3), 21.76 (16, 3H, Tp*-CH_3), 37.43 (21, 2H, Ar-C*H*), 41.74 (6, 1H, Tp*-C*H*), 41.89 (6, 1H, Tp*-C*H*), 49.97 (6, 2H, Ar-C*H*), 66.45 (73, 3H, Tp*-CH_3), 70.73 (16, 3H, Tp*-CH_3). ^{11}B NMR (benzene-d_6, ambient temperature): δ = −83, −76. IR (KBr pellet): $\nu_{B\text{-}H}$ = 2551, 2519 cm^{-1}.

2.1.4. Synthesis of Tp$_2$U[NC(=N-pRPh)-para-cyanobenzene].*

A 20 mL scintillation vial was charged with Tp*$_2$U(N-*p*RPh) (R = OCH_3: 0.200 g, 0.210 mmol; R = CH_3: 0.225 g, 0.240 mmol) in 8 mL THF. To this red solution, an equivalent of terephthalonitrile (R = OCH_3: 0.027 g, 0.210 mmol; R = CH_3: 0.031 g, 0.240 mmol) was added and a slight color change to red-orange was noted. After 30 min, volatiles were removed *in vacuo* which resulted in an orange powder. This powder was washed with *n*-pentane (2 × 5 mL) and dried, affording a pale orange powder (R = OCH_3: 0.184 g, 0.168 mmol, 80% yield; R = CH_3: 0.219 g, 0.203 mmol, 85% yield) assigned as Tp*$_2$U[NC(=N-*p*OMePh)-*p*-cyanobenzene] (**5-OMe**) or Tp*$_2$U[NC(=N-*p*Tolyl)-*p*-cyanobenzene] (**5-Tol**). Single crystals suitable for X-ray crystallographic analysis were obtained from vapor diffusion of concentrated diethyl ether solution into toluene at −35 °C.

2.1.4.1. 5-OMe. Elemental analysis of $C_{46}H_{58}N_{15}B_2OU$: Calculated, C, 50.38; H, 5.33; N, 19.16. Found, C, 50.28; H, 5.14; N, 19.03. ^{1}H NMR (benzene-d_6, ambient temperature): δ = −81.73 (25, 3H, Tp*-CH_3), −78.07 (9, 3H, Tp*-CH_3), −28.48 (3, 1H, Tp*-B*H*), −24.70 (7, 1H, Tp*-B*H*), −20.64 (5, 1H, Tp*-C*H*), −19.91 (4, 1H, Tp*-C*H*), −18.80 (5, 3H, Tp*-CH_3), −14.41 (9, 3H, Tp*-CH_3), −12.31 (4, 3H, Tp*-CH_3), −6.99 (5, 1H, Tp*-C*H*), −5.54 (5, 1H, Tp*-C*H*), −3.50 (3, Tp*-CH_3), 5.46 (5, 3H, -OCH_3), 6.46 (3, 2H, Ar-C*H*), 7.50 (5, 3H, Tp*-CH_3), 15.22 (13, 2H, Ar-C*H*), 19.05 (11, 3H, Tp*-CH_3), 22.70 (11, 3H, Tp*-CH_3), 36.61 (63, 2H, Ar-C*H*), 41.71 (6, 1H, Tp*-C*H*), 41.81 (4, 1H, Tp*-C*H*), 53.06 (81, 2H, Ar-C*H*), 64.32 (742, 3H, Tp*-CH_3), 73.01 (11, 3H, Tp*-CH_3). ^{11}B NMR (benzene-d_6, ambient temperature): δ = −85, −76. IR (KBr pellet): $\nu_{B\text{-}H}$ = 2561, 2520 cm^{-1}; ν_{CN} = 2230 cm^{-1}.

2.1.4.2. 5-Tol. Elemental analysis of $C_{46}H_{58}N_{15}B_2U_1$: Calculated, C, 51.12; H, 5.41; N, 19.44. Found, C, 50.79; H, 5.20; N, 19.17. ^{1}H NMR (benzene-d_6, ambient temperature): δ = −82.78 (12, 3H, Tp*-CH_3), −77.41 (7, 3H, Tp*-CH_3), −27.28 (1, 1H, B-*H*), −25.06 (6, 1H, B-*H*), −20.38 (3, 1H, Tp*-C*H*), −20.31 (3, 1H, Tp*-C*H*), −18.71 (4, 3H, Tp*-CH_3), −18.57 (12, 3H, Tp*-CH_3), −13.88 (11, 3H, Tp*-CH_3), −12.67 (10, 3H, Tp*-CH_3), −7.10 (8, 1H, Tp*-C*H*), −5.87 (9, 1H, Tp*-C*H*), −4.32 (4, 3H, *p*-tolyl-CH_3), −2.99 (11, 1H, Tp*-C*H*), 6.05 (4, 3H, Tp*-CH_3), 7.35 (5, 3H, Tp*-CH_3), 15.57 (9, 2H, C*H*), 20.09 (43, 3H, Tp*-CH_3), 22.04 (10, 3H, Tp*-CH_3), 36.37 (11, 2H, C*H*), 41.86, (10, 1H, Tp*-C*H*), 41.96 (3, 1H, Tp*-C*H*), 53.61 (20, 2H, C*H*), 65.81 (51, 3H, Tp*-CH_3), 70.66 (222, 3H, Tp*-CH_3). ^{11}B NMR (benzene-d_6, ambient temperature): δ = −83, −76. IR (KBr pellet): $\nu_{B\text{-}H}$ = 2557, 2517 cm^{-1}; ν_{CN} = 2227 cm^{-1}.

3. Results and discussion

Because studies were aimed at exploring how reactivity differs with electronic effects of the imido fragment, a U(IV) imido with a *para*-methoxy group was prepared to study in parallel with previously reported Tp*$_2$U(N-*p*Tol) (**2-*p*Tol**). Treating a THF solution of Tp*$_2$UBn (**1-Bn**) with *p*-methoxyphenyl azide leads to immediate effervescence and a color change from dark green to deep red-violet (Scheme 1). Analysis of this red-violet compound by ^{1}H NMR spectroscopy reveals a C_{2v} symmetric spectrum, with seven resonances, including a broad singlet (−20.98 ppm) which is assigned as the Tp* B-H signal and two singlets (18H each) are assigned as the *exo*-(−6.80 ppm) and *endo*-(2.85 ppm) Tp*-CH_3 signals. The pyrazolyl backbone chemical shift is assigned as a singlet (5.48 ppm) which integrates to six protons. The chemical shifts of the aryl protons for the imido substituent are identified as two singlets (52.80 and 77.82 ppm) and methoxy protons are assigned as a singlet at 21.18 ppm. A single resonance is observed by ^{11}B NMR spectroscopy (−66 ppm), which has been seen for other bis(Tp*)U(IV) imido compounds [21]. These data of the red-violet powder are consistent with the assignment as Tp*$_2$U(N-*p*-methoxyphenyl) (**2-OMe**). Alternatively, **2-OMe** can be made from Tp*$_2$UI (**1-I**) with an equiv 4-methoxyphenyl azide and slight excess of KC_8, but in lower yield (83% yield) than the first described method (94% yield). Analysis of **2-OMe** by electronic absorption spectroscopy displays absorptions with low molar absorptivity features throughout the near-infrared (NIR) region, which are consistent with tetravalent uranium complexes (Fig. S4) [19,21]. Efforts to make a U(IV) imido featuring an electron withdrawing group on the aryl ring were unsuccessful. When **1-Bn** is stirred with *para*-nitrophenyl azide, the major product is Tp*$_2$U(O). Reactions of **1-Bn** or **1-I** with 4-trifluoromethylphenyl azide resulted in a mixture of paramagnetic products, including Tp*$_2$-UF_2 and [Tp*$_2$U(N-*p*CF_3Ph)], which could not be separated.

The addition of benzonitrile to **2-OMe** led to a color change from red-violet to red-orange within five minutes; work-up of the reaction mixture afforded an orange powder (Scheme 2). Analysis of a benzene-d_6 solution of this powder by ^{1}H NMR spectroscopy revealed a C_s symmetric spectrum with chemical shifts in the range from −85 to 72 ppm. Twelve chemical shifts corresponding to the methyl group of the two Tp* ligands (3H each) and six shifts (1H each) for the C—*H* of the pyrazolyl rings were noted, as well. Two broad resonances for the B-H of the Tp* ligands are observed at −28.85 and −24.96 ppm. Four chemical shifts equating to two protons each are assigned as aryl protons. A chemical shift worth three protons is also observed at 5.36 ppm, which is attributed to the *para* methoxy group. Two chemical shifts were

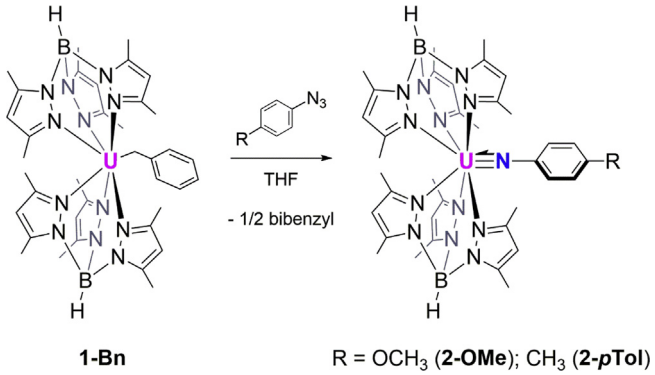

Scheme 1. The synthesis of bis(Tp*)U(IV) imido complexes from **1-Bn**.

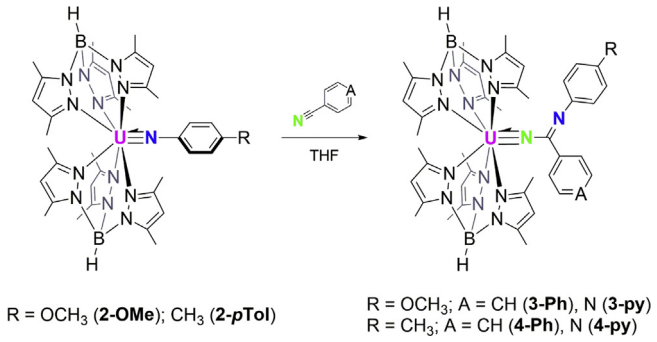

Scheme 2. Synthetic scheme for **3-Ph**, **3-py**, **4-Ph**, and **4-py**.

seen by ^{11}B NMR spectroscopy (−86, −76 ppm), neither of which corresponded to **2-OMe**, suggesting full conversion of the starting material.

To ascertain the identity and coordination mode of the isolated orange powder (79% yield), its molecular structure was elucidated using X-ray crystallography. Analysis of single crystals confirmed the retention of two κ^3-Tp* ligands to a seven-coordinate uranium with U-$N_{pyrazolyl}$ bond distances (2.518(10)–2.701(3) Å) which are similar to other reported bis(Tp*)U compounds (Fig. 1, Table 1) ($Tp^*_2U(CH_3)$ = 2.542(9)–2.700(8) Å [28]; Tp^*_2U(S-Ph) = 2.496(4)–2.674(5) Å [29]; Tp^*_2U(O-Mes) = 2.506(12)–2.697(14) Å [30]). In contrast to prior [2π + 2π] cycloaddition chemistry with actinide imido compounds, the reaction of **2-OMe** with benzonitrile does not result in a κ^2-bound ligand, rather a κ^1-bound amidinate with a new U=N bond is observed, and the previous N-*p*OMePh fragment has a newly formed C=N bond. The bond distance of the new U–N bond (2.004(3) Å) is consistent with reported U(IV) imido bond lengths (tBu$_2$bpy)UI_2(N-tBu)(THF)$_2$ = 1.931(5) Å [31]; $Cp^PU(^{Mes}PDI^{Me})$(N-dipp) (Cp^P = 1-(7,7-dimethylbenzyl)cyclopentadienide; $^{Mes}PDI^{Me}$ = 2,6-((Mes)N = CMe)$_2C_5H_3N$) = 1.984(4) Å [32]; Tp^*_2U(N-*p*Tol) = 2.011(9) Å [21]). The U—N—C bond angle (178.1(2)°) is nearly linear, which is consistent with bisTp^*U(IV) imido compounds (Tp^*_2U(N-Bn) = 165.7(2)°; Tp^*_2U(N-2,6-diethylphenyl) = 173.8(9)°) [21]. The bond lengths corresponding to the remainder of the amidinate fragment show inequivalent N—C bond distances, where N13–C31 (1.357(4) Å) is slightly longer than N14–C31 (1.305(5) Å), which can be assigned to the η^1-amidinate ligand, N—C(=N-*p*OMePh)Ph. Overall, the product of **2-OMe** with benzonitrile is assigned as Tp^*_2U[=N—C(=N-*p*OMePh)Ph (**3-Ph**).

A previous example of benzonitrile reacting with an actinide imido was reported by Zi and co-workers. Treatment of [η^5-1,2,4-$(Me_3C)_3C_5H_2]_2$Th(N-*p*Tol) with benzonitrile resulted in a κ^2-binding mode to a Th(IV) center [15]. Amidinate ligands have been employed with actinide complexes before, but those reported have bound through both nitrogen atoms of the ligand [33]. At the time of submission, there were no other reported compounds with such a κ^1-binding motif as seen with **3-Ph**.

To study any effect of any heteroatom incorporation, **2-OMe** was treated with 4-cyanopyridine, which also produced a color change to red-orange. The pale orange powder obtained from work-up (83% yield) was analyzed by ^{1}H NMR spectroscopy as a benzene-d_6 solution, and showing similar resonance distribution with chemical shifts in the range of −81–73 ppm and pattern to **3-Ph**. This similar compound is assigned as **3-py**, which also features two chemical shifts in its ^{11}B NMR spectrum (−86, −75 ppm) in the same region as **3-Ph**. Molecular structure of orange **3-py** was confirmed by X-ray diffraction, showing a seven-coordinate uranium ion with the same η^1-bonding of the

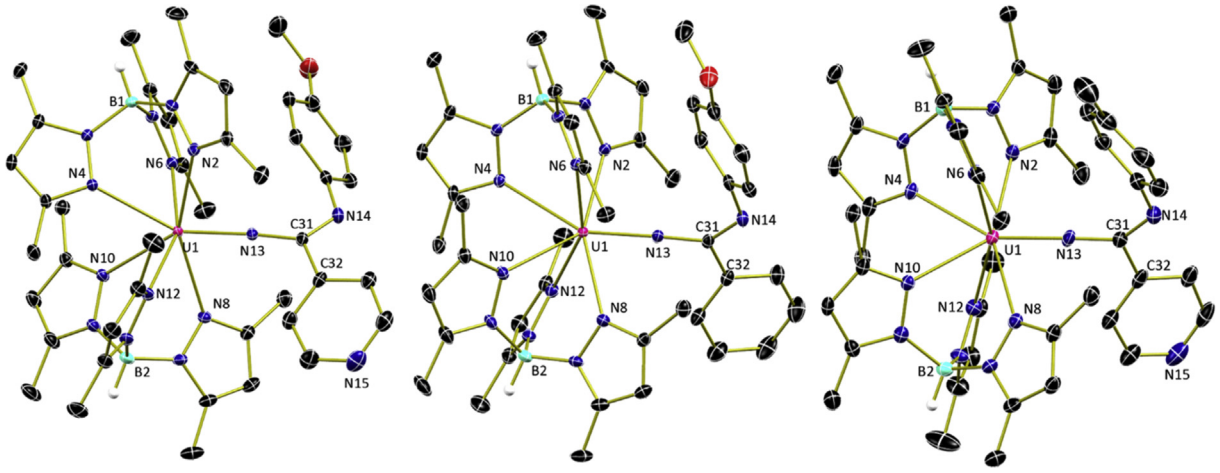

Fig. 1. Molecular structures of **3-py**, **3-Ph**, and **4-py** (left to right) displayed with 30% probability ellipsoids. Any co-crystallized molecules and selected hydrogen atoms have been omitted for clarity.

Table 1
Selected bond lengths and bond angles of **3-Ph**, **3-py**, **4-py**, **5-OMe**, and **5-Tol**.

	3-Ph	3-py	4-py	5-Tol	5-OMe
U–$N_{pyrazolyl}$	2.518(3)–2.701(3) Å	2.524(2)–2.690(2) Å	2.510(4)–2.687(4) Å	2.512(6)–2.776(5) Å	2.515(4)–2.674(4) Å
U–N13	2.004(3) Å	2.012(2) Å	2.013(4) Å	2.019(6) Å	2.047(5) Å
N13–C31	1.357(4) Å	1.354(3) Å	1.362(6) Å	1.346(8) Å	1.300(7) Å
C31–C32	1.494(5) Å	1.507(4) Å	1.528(7) Å	1.503(9) Å	1.522(7) Å
C31–N14	1.305(5) Å	1.302(3) Å	1.296(7) Å	1.318(8) Å	1.314(7) Å
U1–N13–C31	178.1(2)°	175.92(17)°	177.6(4)°	174.8(4)°	175.9(4)°

amidinate as **3-Ph** (Fig. 1, left; Table 1). The molecular structure of **3-py** has U–$N_{pyrazolyl}$ distances (2.524(2)–2.690(2) Å) in a range similar to **3-Ph**. An imido fragment, identified as κ^1-amidinate N—C(=N-*p*OMePh)pyr, is κ^1-bound through a nitrogen atom with a short U-N bond distance of 2.012(2) Å, which signifies a U(IV) imido. Additionally, **3-py** features a linear U—N—C bond angle (175.92(17)°) within its amidinate fragment.

To determine if electronic changes in uranium imido play any role in product formation, the methyl-substituted aryl imido, **2-*p*Tol**, was treated with benzonitrile and 4-cyanopyridine. Both reagents gave a color change from red-violet to red-orange. Upon work-up, orange powders were isolated and assigned as **4-Ph** (75% yield) and **4-py** (78% yield) (Scheme 2). Both iterations have ^{1}H and ^{11}B NMR and IR spectra similar to their *p*-OMe substituted counterparts. For confirmation of the molecular structure, **4-py** was analyzed using X-ray diffraction (Fig. 1, right). Data refinement shows a seven-coordinate uranium center with two κ^3-Tp* ligands with U-N bond distances that are similar to **3-py** and **3-Ph** (Table 1), as well as formation of a κ^1-amidinate with the formula —NC(=N-*p*-Tol)pyr. This U—N bond length (2.013(4) Å) is similar to the other discussed U-N bond lengths in this report.

Compounds **3-Ph**, **3-py**, **4-Ph**, and **4-py** display similar features in their electronic absorption spectroscopic profiles (Fig. 2). The near-infrared (NIR) region has low molar absorptivity f-f transitions throughout, which are consistent with U(IV), f^2 configuration [34]. All four of these compounds also display a local λ_{max} (about 500 nm) that corresponds to their pale orange color.

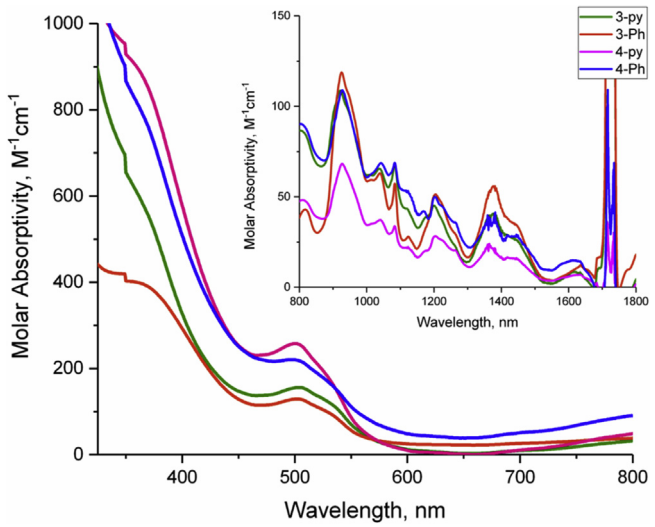

Fig. 2. Electronic absorption spectra of **3-py** (green), **3-Ph** (orange), **4-py** (pink), and **4-Ph** (blue) recorded from 300 to 1800 nm in THF at ambient temperature. (Colour online.)

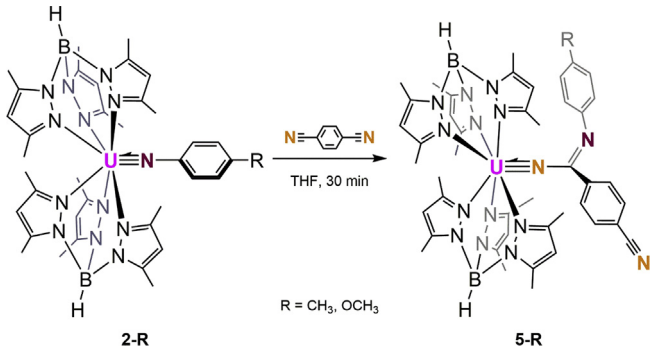

Scheme 3. Synthetic scheme for **5-OMe** and **5-Tol**.

The formation of dinuclear species was attempted by adding one-half an equivalent of 1,4-dicyanobenzene to a stirring solution of **2-*p*Tol** in THF, which caused a slight color change from red to red-orange (Scheme 3). After work-up, an orange powder was isolated (85% yield) and analyzed as a C_6D_6 solution by ^{1}H NMR spectroscopy. As noted with the other nitrile reactions, a C_S symmetric NMR spectrum with resonances in the range of −83–71 ppm was observed. Further analysis of the orange powder by infrared spectroscopy (KBr) showed two absorptions assignable to the B-H stretches (2517, 2557 cm^{-1}) of the Tp* ligands. A strong absorption at 2227 cm^{-1} was also present, indicating a nitrile functional group was still intact, inconsistent with formation of a dinuclear species.

To further probe the molecular structure, crystals of **5-Tol** grown from vapor diffusion of a concentrated diethyl ether solution into toluene and analyzed by X-ray diffraction. This technique provided confirmation that two Tp* ligands were coordinated to a pentagonal bipyramid uranium center (Fig. 3, left). The U—$N_{pyrazole}$ bond lengths (2.512(6)–2.776(5) Å) are similar to the previously discussed compounds (Table 1). Crystallography also revealed formation of a κ^1-amidinate ligand, with a short U—N bond length of 2.019(6) Å, which is in the range of other U—N multiple bond lengths presented here. The U—$N_{amidinate}$—C bond angle is nearly linear at 174.8(4)°. When examining bond distances further, N13–C31 (1.346(8) Å) and N15–C31 (1.318(8) Å) are within range for the other compounds (Table 1). The C—N bond length (1.147 (10) Å) indicates that there has not been any reduction or activation of the second nitrile group. This confirmation allows for the assignment as Tp$^*_2$U(=N—C(=N-*p*Tol)-*p*-cyanobenzene (**5-Tol**). Compound **5-Tol** was also probed by electronic absorption spectroscopy, which displayed characteristic weak absorbances in the NIR region (Fig. S19) similar to those present for compounds **3** and **4**. The UV–Vis region displays an absorbance at 515 nm, which likely gives **5-Tol** its red-orange color. This result contrasts work from Kiplinger and co-workers who used 1,4-dicyanobenzene to prepare bimetallic actinide complexes through nitrile insertion chemistry, which gave a bridging diketimide product. [$(C_5H_4Et)_2$(Cl)U]$_2$(μ-[N=C—(CH_3)—C_6H_4—(CH_3)C=N]) [35].

Studying 1,4-dicyanobenzene with **2-OMe** provides another opportunity to track reactivity using different electronic groups. Similar to the reaction to yield **5-Tol**, an orange powder is isolated upon workup (80% yield), which has a C_S symmetric ^{1}H NMR spectrum (C_6D_6, ambient temperature) with 24 resonances ranging from −82 to 72 ppm. This orange powder also displays three notable stretches by IR spectroscopy; two absorbances correspond with the B–H of Tp* (2561, 2520 cm^{-1}) and a strong stretch (2230 cm^{-1}) is assigned to a nitrile functional group. The similar spectroscopic data gives the assignment of the orange powder as Tp$^*_2$U[NC(=N-*p*OMePh)-*p*-cyanobenzene] (**5-OMe**).

An examination of **5-OMe**'s molecular structure was studied using X-ray crystallography (grown from a concentrated diethyl ether solution at −35 °C) (Fig. 3, right). A pentagonal bipyramid uranium ion with two bound κ^2-Tp* ligands with U—$N_{pyrazolyl}$ bond lengths (2.515(4)–2.674(4) Å) that are similar to **5-Tol** (Table 1). Confirmation of the same κ^1-amidinate ligand was also observed by crystallography, with U—$N_{amidinate}$ (2.047(5) Å) and U—N—C (175.9(4)°) within range of the four κ^1-amidinate complexes presented (Table 1). The C—$N_{nitrile}$ bond length (1.143(9) Å) shows no activation at the second nitrile, just like **5-Tol**.

Formation of the new amidinate ligands for **3-Ph**, **3-py**, **4-Ph**, **4-py**, **5-OMe**, and **5-Tol** likely occurs from a [2π + 2π] cycloaddition event between the imido fragment and the incoming nitrile (**I** in Fig. 4), which leads to a metalacyclic product, **II**. From here, [2π+2π]-cycloreversion of the C=N bond of the added nitrile fragment and the U—N bond of the starting imido continues, generating the κ^1-amidinate products. Thus, the work in this article diverges from previous examples, such as Boncella's imido

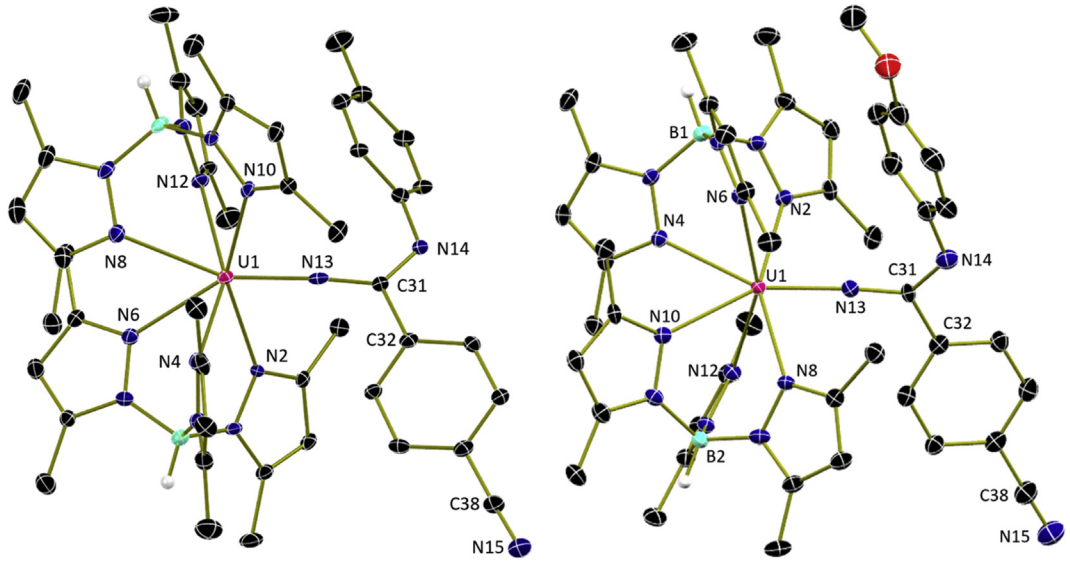

Fig. 3. Molecular structures of **5-Tol** (left) and **5-OMe** (right) shown with 30% probability ellipsoids. Selected hydrogen atoms and co-crystalized solvent molecules have been omitted for clarity.

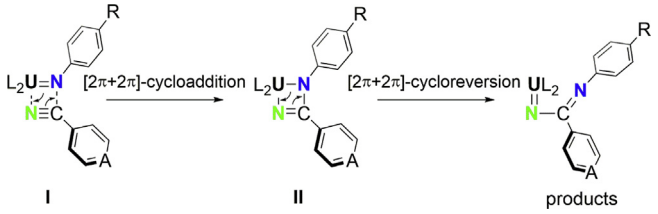

Fig. 4. Proposed mechanistic pathway for product formation.

group switching [16] or Zi's Th example leading to a κ^2-bound ligand [15].

4. Conclusions

Overall, we have demonstrated that bis-Tp*U(IV) amidinate compounds can be synthesized from [2π + 2π]-cycloaddition and [2π + 2π]-cycloreversion of uranium(IV) imido compounds with nitriles. This is successful regardless for both imido groups (methyl versus methoxy) or the type of nitrile employed. Full characterization of these compounds using multinuclear NMR, infrared, and electronic absorption spectroscopies, with the aid of X-ray crystallography, confirmed the unanticipated κ^1-coordination of the amidinate ligands as well as their tetravalent nature.

Interestingly, the imido reactivity observed here diverges from what has been reported. Using nitriles sees these imidos undergo consecutive multiple bond metathesis pathways, rather than just one, yielding new sterically hindered amidinates not typically observed in cycloaddition chemistry.

Acknowledgements

This work was supported by the National Science Foundation (CHE-1665170, SCB). The X-ray crystallographic data in this work was obtained on instruments funded by the NSF through the Major Research Instrumentation Program (CHE-1625543).

Appendix A. Supplementary data

CCDC 1852446, 1854084, 1854085, 1854086, 1873214 contains the supplementary crystallographic data for **5-Tol**, **4-py**, **3-Ph**, **3-py**, **5-OMe**. These data can be obtained free of charge via http://www.ccdc.cam.ac.uk/conts/retrieving.html, or from the Cambridge Crystallographic Data Centre, 12 Union Road, Cambridge CB2 1EZ, UK; fax: (+44) 1223-336-033; or e-mail: deposit@ccdc.cam.ac.uk.

Supplementary data to this article can be found online at https://doi.org/10.1016/j.poly.2018.10.042.

References

[1] A.R. Fox, S.C. Bart, K. Meyer, C.C. Cummins, Towards uranium catalysts, Nature 455 (2008) 341.
[2] H.S. La Pierre, K. Meyer, Activation of small molecules by molecular uranium complexes, in: K.D. Karlin (Ed.), Progress in Inorganic Chemistry, John Wiley & Sons, 2014, pp. 303–415.
[3] S.T. Liddle, The renaissance of non-aqueous uranium chemistry, Angew. Chem. Int. Ed. Engl. 54 (2015) 8604.
[4] T.W. Hayton, Metal-ligand multiple bonding in uranium: structure and reactivity, Dalton Trans. 39 (2010) 1145.
[5] T.W. Hayton, Recent developments in actinide-ligand multiple bonding, Chem. Commun. 49 (2013) 2956.
[6] A. Haskel, T. Straub, M.S. Eisen, Organoactinide-catalyzed intermolecular hydroamination of terminal alkynes, Organometallics 15 (1996) 3773.
[7] T. Straub, A. Haskel, T.G. Neyround, M. Kapon, M. Botoshansky, M.S. Eisen, Intermolecular hydroamination of terminal alkynes catalyzed by organoactinide complexes. Scope and mechanistic studies, Organometallics 2001 (2001) 5017.
[8] G. Zi, L.L. Blosch, L. Jia, R. Andersen, Preparation and reactions of base-free bis (1,2,4-tri-*tert*-butylcyclopentadienyl)uranium methylimide, Cp'$_2$U=NMe, and related compounds, Organometallics 24 (2005) 4602.
[9] W. Ren, G. Zi, D.C. Fang, M.D. Walter, Thorium oxo and sulfido metallocenes: synthesis, structure, reactivity, and computational studies, J. Am. Chem. Soc. 133 (2011) 13183.
[10] C. Zhang, P. Yang, E. Zhou, X. Deng, G. Zi, M.D. Walter, Reactivity of a Lewis base supported thorium terminal imido metallocene toward small organic molecules, Organometallics 36 (2017) 4525.
[11] R.E. Jilek, N.C. Tomson, B.L. Scott, J.M. Boncella, [2 + 2] cycloaddition reactions at terminal imido uranium(IV) complexes to yield isolable cycloadducts, Inorg. Chim. Acta 422 (2014) 78.
[12] S.C. Bart, C. Anthon, F.W. Heinemann, E. Bill, N.M. Edelstein, K. Meyer, Carbon dioxide activation with sterically pressured mid- and high-valent uranium complexes, J. Am. Chem. Soc. 130 (2008) 12536.
[13] W. Ren, E. Zhou, B. Fang, G. Hou, G. Zi, D.C. Fang, M.D. Walter, Experimental and computational studies on the reactivity of a terminal thorium imidometallocene towards organic azides and diazoalkanes, Angew. Chem. Int. Ed. Engl. 53 (2014) 11310.
[14] W. Ren, E. Zhou, B. Fang, G. Zi, D.-C. Fang, M.D. Walter, Si–H addition followed by C–H bond activation induced by a terminal thorium imido metallocene: a combined experimental and computational study, Chem. Sci. 5 (2014).
[15] W. Ren, G. Zi, D.C. Fang, M.D. Walter, A base-free thorium-terminal-imido metallocene: synthesis, structure, and reactivity, Chem. Eur. J. 17 (2011) 12669.

[16] L.P. Spencer, P. Yang, B.L. Scott, E.R. Batista, J.M. Boncella, Imido exchange in bis (imido) uranium(VI) complexes with aryl isocyanates, J. Am. Chem. Soc. 130 (2008) 2930.
[17] K.P. Kepp, A quantitative scale of oxophilicity and thiophilicity, Inorg. Chem. 55 (2016) 9461.
[18] G. Zi, L. Jia, E.L. Werkema, M.D. Walter, J.P. Gottfriedsen, R.A. Andersen, Preparation and reactions of base-free bis(1,2,4-tri-tert-butylcyclopentadienyl)uranium oxide, Cp'$_2$UO, Organometallics 24 (2005) 4251.
[19] E.M. Matson, M.P. Crestani, P.E. Fanwick, S.C. Bart, Synthesis of U(IV) imidos from Tp*$_2$U(CH$_2$Ph) (Tp* = hydrotris(3,5-dimethylpyrazolyl)borate) by extrusion of bibenzyl, Dalton Trans. 41 (2012) 7952.
[20] E.M. Matson, P.E. Fanwick, S.C. Bart, Diazoalkane reduction for the synthesis of uranium hydrazonido complexes, Eur. J. Inorg. Chem. 2012 (2012) 5471.
[21] C.J. Tatebe, M. Zeller, S.C. Bart, [2pi+2pi] cycloaddition of isocyanates to uranium(IV) imido complexes for the synthesis of U(IV) kappa(2)-ureato compounds, Inorg. Chem. 56 (2017) 1956.
[22] A.B. Pangborn, M.A. Giardello, R.H. Grubbs, R.K. Rosen, F.J. Timmers, Safe and convenient procedure for solvent purification, Organometallics 15 (1996) 1518.
[23] C. Soma, C. Jayanta, G. Wenhua, B.W. Edward, Functionalization of potassium graphite, Angew. Chem. Int. Ed. 46 (2007) 4486.
[24] Y. Sun, R. McDonald, J. Takats, V.W. Day, T.A. Eberspacher, Synthesis and structure of bis[hydrotris(3,5-dimethylpyrazolyl)borato]iodouranium(III), U[HB(3,5-Me$_2$pz)$_3$]$_2$I: unprecedented side-on interaction involving a hydrotris (pyrazolyl)borate ligand, Inorg. Chem. 33 (1994) 4433.
[25] E.M. Matson, W.P. Forrest, P.E. Fanwick, S.C. Bart, Functionalization of carbon dioxide and carbon disulfide using a stable uranium(III) alkyl complex, J. Am. Chem. Soc. 133 (2011) 4948.
[26] K. Barral, A.D. Moorhouse, J.E. Moses, Efficient conversion of aromatic amines into azides: a one-pot synthesis of triazole linkages, Org. Lett. 9 (2007) 1809.
[27] B. AXS, APEX3, Bruker AXS Inc, Madison, WI, 2016.
[28] E.M. Matson, W.P. Forrest, P.E. Fanwick, S.C. Bart, Use of alkylsodium reagents for the synthesis of trivalent uranium alkyl complexes, Organometallics 31 (2012) 4467.
[29] E.M. Matson, P.E. Fanwick, S.C. Bart, Formation of trivalent U–C, U–N, and U–S bonds and their reactivity toward carbon dioxide and acetone, Organometallics 30 (2011) 5753.
[30] M.A. Antunes, Â. Domingos, I.C.D. Santos, N. Marques, J. Takats, Synthesis and characterization of uranium(III) compounds supported by the hydrotris(3,5-dimethyl-pyrazolyl)borate ligand: Crystal structures of [U(TpMe$_2$)$_2$(X)] complexes (X=OC$_6$H$_2$-2,4,6-Me$_3$, dmpz, Cl), Polyhedron 24 (2005) 3038.
[31] R.E. Jilek, L.P. Spencer, D.L. Kuiper, B.L. Scott, U.J. Williams, J.M. Kikkawa, E.J. Schelter, J.M. Boncella, A general and modular synthesis of monoimidouranium(IV) dihalides, Inorg. Chem. 50 (2011) 4235.
[32] J.J. Kiernicki, C.J. Tatebe, M. Zeller, S.C. Bart, Tailoring the electronic structure of uranium mono(imido) species through ligand variation, Inorg. Chem. 57 (2018) 1870.
[33] C.E. Hayes, D.B. Leznoff, Actinide coordination and organometallic complexes with multidentate polyamido ligands, Coord. Chem. Rev. 266–267 (2014) 155.
[34] I. Castro-Rodriguez, K. Meyer, Small molecule activation at uranium coordination complexes: control of reactivity via molecular architecture, Chem. Commun. (2006) 1353.
[35] E.J. Schelter, J.M. Veauthier, C.R. Graves, K.D. John, B.L. Scott, J.D. Thompson, J.A. Pool-Davis-Tournear, D.E. Morris, J.L. Kiplinger, 1,4-dicyanobenzene as a scaffold for the preparation of bimetallic actinide complexes exhibiting metal-metal communication, Chem. Eur. J. 14 (2008) 7782.